

## Effect of Mandibular Inclination on CBCT Artifact Presented in Endodontically-Treated Teeth

Kanokwan Wiwatcharoen<sup>1</sup>, Sirilawan Tohnak<sup>2</sup>, Chutamas Deepho<sup>2</sup>, Adjabhak Wongviriya<sup>2</sup>,  
Kittipong Ketpan<sup>1</sup>, Peraya Puapichartdumrong<sup>1</sup>, Khemjira Jarassri<sup>1</sup>,  
Kasidid Ruksakiet<sup>1</sup>, Kessiri Wisithphrom<sup>1\*</sup>

1. Department of Restorative Dentistry, Faculty of Dentistry, Naresuan University, Phitsanulok 65000, Thailand.  
2. Department of Oral Diagnosis, Faculty of Dentistry, Naresuan University, Phitsanulok, 65000, Thailand.

### Abstract

This study evaluated the influence of mandibular inclination and artifact patterns in CBCT images of endodontically-treated teeth by employing novel assessment systems.

Eleven endodontically-treated teeth were scanned using CBCT at 0-, 5-, 10-, 15-, and 20-degree mandibular tilting. The streak artifact was assessed on coronal, middle, and apical thirds using a 4-point score to classify the hypodense line artifact in eight directions and calculating the change of pixel intensity value percentile in the histogram graph. The correlation between inclinations and artifact patterns was analyzed using logistic regression.

The mandibular inclination unaffected the artifact pattern in the coronal third using scoring system, but there was an impact in the middle and apical third on mesial ( $p=0.02$ ,  $p<0.01$ ) and distal direction ( $p<0.01$ ,  $p<0.01$ ), respectively of endodontically-treated teeth. In the quantifying system assessment, tilting the mandible backward at 10- ( $p=0.04$ ) and 15-degree ( $p=0.02$ ) increased the probability of creating artifacts in the middle third by approximately 3.61 and 4.42 times, respectively. The artifact predominantly presented in the coronal (mesial,  $p<0.01$  and distal,  $p<0.01$ ) and middle third (distal,  $p<0.01$ ) but absent in the apical third of the root.

Tilting the head backward at 10- and 15-degree increased artifact presentation in the cross-direction image of endodontically-treated teeth.

**Clinical article (J Int Dent Med Res 2024; 17(1): 283-290)**

**Keywords:** Tilting head, mandibular inclination, CBCT, endodontically-treated teeth, artifact.

**Received date:** 02 January 2024

**Accept date:** 11 March 2024

### Introduction

Cone-beam computed tomography (CBCT) is suggested as a modality for detecting vertical root fracture (VRF).<sup>1,2</sup> CBCT images of endodontically-treated teeth show a wide range of artifact variations. High-density root canal filling materials and the specific scanning parameters used in CBCT cause imaging abnormalities, such as hypodense lines and enlarged root canal dimensions.<sup>3-7</sup> Surprisingly, despite claims of improved image quality, applying the metal artifact reduction algorithms in CBCT scans of endodontically-treated teeth with VRF hindered it.<sup>3,8,9</sup> Many studies have attempted to adjust the CBCT scanning

parameters alterations, including tube current (mA), tube voltage (kVp), resolution (voxel size), and field of view (FOV), to provide a better radiographic interpretation and reduce artifacts from materials.<sup>4-7,10,11</sup> However, adjusting the mentioned parameters is insufficient to eliminate artifacts in CBCT images without quality degradation.<sup>12</sup>

The patient's head position may also impact the number of tissues that cone-shaped x-ray photons pass through before reaching the detectors.<sup>12</sup> In endodontically-treated teeth, filling materials absorb x-ray photons in a single plane of the projecting image and cause the most pronounced artifacts.<sup>10</sup> Adjusting the patient's head position can prevent the overlapping of high-density materials in the inter-plane image.<sup>13</sup> Several studies showed a successful improvement of CBCT image quality by tilting the head position in either a forward or backward direction.<sup>12-14</sup> However, the effect of mandibular inclination on the inter-plane artifacts of endodontically-treated teeth is questionable.

#### \*Corresponding author:

Associated Professor Dr. Kessiri Wisithphrom DDS, PhD  
Department of Restorative Dentistry, Faculty of Dentistry,  
Naresuan University, Phitsanulok 65000, Thailand  
E-mail: [kessiriw@nu.ac.th](mailto:kessiriw@nu.ac.th), [kessiri\\_kate@yahoo.com](mailto:kessiri_kate@yahoo.com)

A comprehensive technique to identify artifacts in CBCT images are subjective and objective methods.<sup>15</sup> In the subjective method, the observers characterize the artifact severity or pattern based on their decision. The objective method, such as the grayscale and contrast-noise-ratio (CNR) analysis, provides quantitative data through reproducible techniques. The grayscale analysis is a common approach to measuring mean pixel intensity within the defining regions of interest (ROIs).<sup>4,6,15,16</sup> Another objective method, CNR analysis, defines the ratio of gray value difference to image noise level and reported as the mean CNR. Low CNR values indicated a large number of artifacts. However, the limitations of CNR analysis are CNR values can vary depending on CBCT equipment, ROI placement, and the artifact types observed in different study settings.<sup>17-19</sup> The grayscale and CNR analysis are widely used, but their sensitivity and specificity in detecting streaking artifacts in the CBCT images remained unclear.

As previously mentioned, the patient head's position might influence the presence of the artifact. However, there is limited study on the role of tilting the mandible in reducing artifacts in endodontically-treated teeth. This study aimed to investigate the influence of mandibular inclination on artifact formation and introduced a methodology for artifact characterization and quantification with novel scoring and quantifying systems.

## Materials and methods

This study was carried out after ethical approval from the University Institutional Review Board and performed at the University Dental Hospital. The sample size was calculated at 80% power of the test and 95% confidence level using G\*Power version 3.1.9.7 (Franz Faul, University Kiel, Germany). The minimal number of samples was 55 from five groups and eleven teeth per group of endodontically-treated mandibular left second premolars.

### Sample selection and preparation

This study included the permanent mandibular left second premolars that were extracted for orthodontic purposes. All teeth were required to have complete single root canal formation without root restorations and pathology from caries, root resorption, cracks, or fractures. After gathering, samples were disinfected with

5.25% sodium hypochlorite (NaOCl). Coronal part of each tooth was sectioned using a diamond disc (Edenta, Switzerland). The working length was determined using K-file no. 10 (Dentsply Sirona, Switzerland). Root canals were prepared using ProTaper Gold rotary files (Dentsply Sirona, Switzerland) following protocols: size/taper: 19/04, 18/02, 20/04, 20/07, 25/08, 30/09, and 40/06. Irrigation of the canal was performed using a 2.5% NaOCl solution and final rinse with 2.5% NaOCl 17% Ethylenediaminetetraacetic acid and distilled water. The root canal filling was performed using the continuous wave technique with a matched gutta percha cone (Dentsply Sirona, Switzerland) and AH Plus sealer (Dentsply Sirona, Switzerland).

### CBCT acquisition

A 3D-printed model secured the base of the human mandible at each desired inclination. The mandibular occlusal plane was positioned parallel to the horizontal plane. (Figure 1)

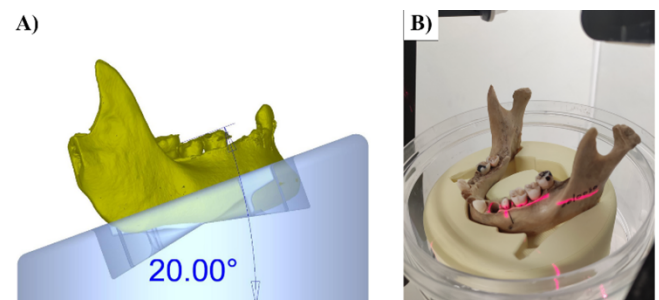


**Figure 1.** Sample aligning devices and position for CBCT scan. **A)** The design of the 3D printing platform that fits the mandible base to place the mandible 20-degree. **B)** Positions of the specimen during a CBCT scan.

The samples were prepared and inserted into the mandible before being scanned using a Veraview X800 CBCT machine (J Morita Mfg. Corp., Japan). The scanning process was performed at five distinct anteroposterior inclinations: 0-, 5-, 10-, 15-, and 20-degree. The exposure parameters were as follows: 90 kVp, 2 mA, a 4 x 4-cm FOV, a 0.08-mm voxel size, and a 360-degree scan projection. The CBCT data were reconstructed using the accompanying acquisition software, i-Dixel 2.0 (J Morita Mfg. Corp., Japan). The root of each tooth was divided into three equal segments: coronal, middle, and apical thirds. The axial view images were exported as Bitmap files for interpretation.

### The scoring system

A 14-inch in-plane switching screen with a maximum resolution of 2,160×1,440 pixels was used to ensure consistent lighting throughout the evaluation. This study modified likubo's 4-point score to classify the presence of the hypodense line artifact.<sup>10</sup> A linear dark area with a thickness measuring less than 0.5 mm was defined as a hypodense line artifact. The hypodense line artifact was classified based on likubo's original scores: scores 0, indicating the absence of a line, and 1, indicating an unclear line, were categorized as "absent," while scores of 2, indicating a distinct line without root penetration, and 3, indicating a line that penetrates the root, were classified as "present". Hypodense lines were assessed in each ROI to determine the artifact's direction in relation to the root canal filling materials. These ROIs corresponded to eight distinct directions, comprising four cross-directions (buccal, mesial, lingual, distal) and four oblique directions (mesiobuccal, mesiolingual, distolingual, distobuccal). This comprehensive scoring approach ensured a thorough examination of the hypodense line artifact from various perspectives, enhancing the precision and completeness of the analysis.

### Quantifying system

The axial view CBCT images were analyzed using ImageJ version 1.8.0 (Figure 2A).<sup>20</sup> Initially, the original CBCT images were enlarged four times using the Resize\_Roi plugin created by Maugeri Chiara and Virzi Emanuela (2011). The root of the mandibular left second premolar was selected and cropped to a size of 453×453 pixels (Figure 2B). The root canal filling material region was segmented using Minimal's thresholding method.<sup>21</sup> The Feret diameter, the longest distance between any two points, of the root canal filling materials were located and used as a reference line in the buccolingual direction (Figure 2C). An eight-directional asterisk image was created to represent eight directions (Figure 2D). Three images, including the original image, root canal filling material with Feret diameter, and asterisk image, were merged in different color channels (Figure 2E). The composite channel was converted to RGB. The RGB planes plugin created by Gabriel Landini (2007) was used to align the vertical line of the asterisk image to superimpose with the Feret diameter of the root canal filling material image (Figure 2F).

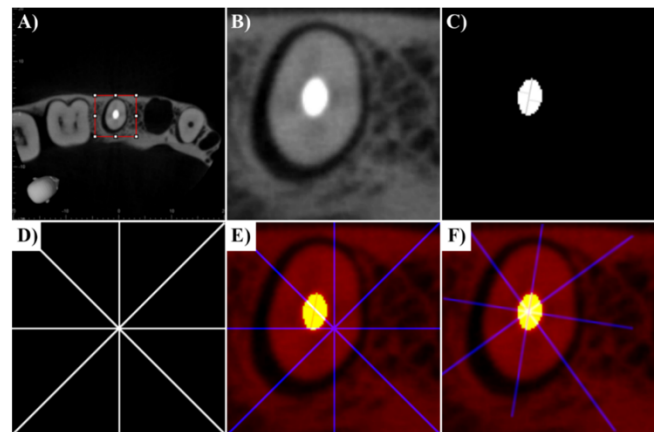


**Figure 2.** The determination of streak artifact using quantifying system on ImageJ software. **A)** ROI was selected. **B)** Cropped image of the original image. **C)** Area of the root canal filling materials region was selected and draw the Feret and Breadth **D)** Eight directions asterisk image. **E)** image B), C) and D) were merged into a composite channel. **F)** The vertical line of the asterisk channel was aligned to superimpose with the Ferret line.

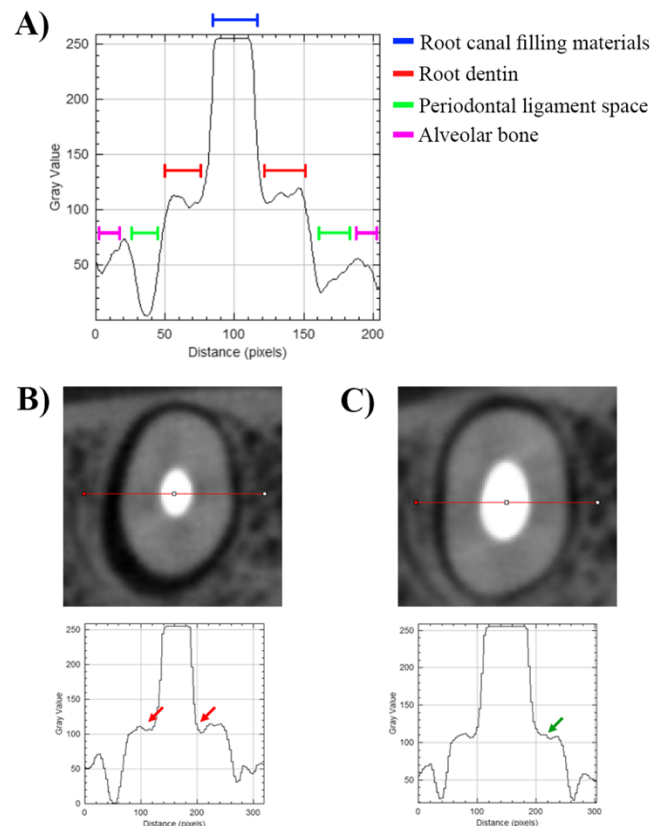


**Figure 3.** The histogram graph interpretation **A)** the histogram graph shows three intensity peaks representing the intensity values of alveolar bone, root dentin, and root canal filling materials **B)** Example of sample which had a streak artifact.

On the histogram graph from the mesiodistal line of a CBCT image of an endodontically-treated tooth, a streak artifact was detected (red arrow). **C)** Example of sample which had a hypodense line artifact. On the histogram graph from the mesiodistal line of a CBCT image of an endodontically-treated tooth, a streak artifact was undetected (green arrow).

The composite channel was then split, and the Feret diameter of the root canal filling material image was closed. The original image and the aligned asterisk image were used to create a stack. A straight line was drawn buccolingually with the guide from the eight-direction line on the asterisk window before switching the window to the original image window. Subsequently, intensity along the selected line was determined using profile plot command. This process was repeated in other directions: mesiobuccal-distolingual, mesiodistal, and mesiolingual-distobuccal directions.

An analysis of the plot between the pixel intensity and distance determines the presence of artifacts (Figure 3). The intensity observed at the interface between root dentin and root canal filling material was categorized as follows: a drop less than 10% of intensity compared to root dentin intensity signified no streak artifact, while a 10% drop or more indicated the presence of a streak artifact (Figure 3B).<sup>22</sup>

**Statistical analysis**

All data was statistically analyzed using IBM SPSS statistical analysis software version 26 (IBM Corp., USA). The inter- and intra-observer agreement was determined using weighted kappa coefficients. Only a kappa coefficient  $\geq 0.81$  was considered acceptable.<sup>23</sup> The probability of artifact presence at each root level, the correlation between mandibular inclination, and the direction of artifact presentation analyzed with Logistic regression. The *p*-value  $< 0.05$  was considered a significant difference.

**Results**

**The determination of the artifact presentation using the scoring system**

Following the attainment of inter- and intra-observer agreement, this study assessed the factors influencing artifact presence. Among 165 CBCT segments from 55 samples, the apical

third exhibited 2.74 times (74 artifacts) and the middle third 1.74 times (47 artifacts) more artifacts than the coronal third (27 artifacts). Examining mandibular inclination in the coronal third, the highest artifact frequency occurred at 10- and 15-degree (7 artifacts), followed by 0-, 20-, and 5-degree (5, 5, 3 artifacts, respectively). In the middle third, the highest frequency was at 20-degree (13 artifacts), followed by 10-, 5-, 0-, and 15-degree (12, 10, 7, 5 artifacts, respectively). The apical third exhibited the highest frequency at 20-degree (18 artifacts), followed by 0-, 10-, 15-, and 5-degree (17, 15, 14, 10 artifacts, respectively). Across all root levels, artifacts predominantly occurred in the cross-direction as shown in Figure 4.

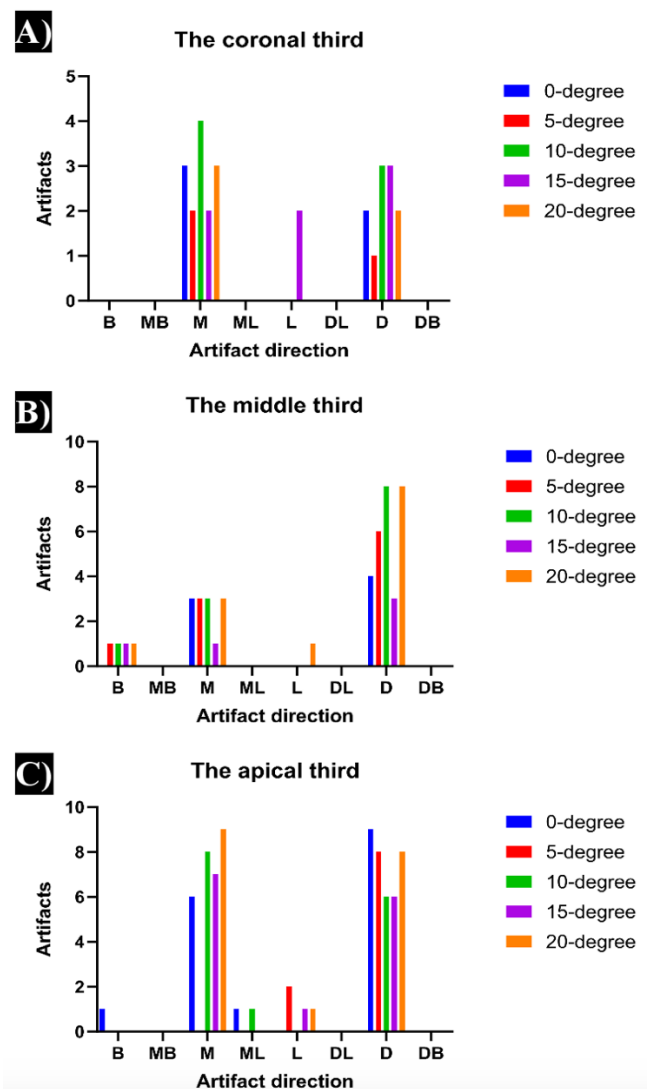


**Figure 4.** The frequency distribution of artifact presentation using the scoring system **A)** The coronal third **B)** The middle third and **C)** The apical third.



While neither direction nor inclination influenced artifacts in the coronal third, logistic regression revealed significant influences in the middle and apical thirds. In the middle third, artifact occurrence in the mesial and distal directions was 4.12 and 16.25 times higher than in the buccal direction, respectively. In the apical third, artifact occurrence in the mesial and distal directions was 26.59 times higher than in the buccal direction.

The kappa coefficient for inter-observer agreement reached a substantial level at 0.75, and intra-observer agreements for the radiologist and endodontist were substantial at 0.76 and 0.70, respectively.

**The determination of the artifact presentation using the quantifying system**

The distribution of the artifact presentation at each root level is shown in Figure 5, with the coronal third presented 22.6 times (113 artifacts) and the middle third presented 9.6 times (48 artifacts) higher than the apical third (5 artifacts), respectively. Regarding the mandibular inclination, in coronal third, the highest frequency artifact was presented at 0- and 20-degree (26 artifacts), followed by 5-, 15- and 10-degree (25, 19, 17 artifacts, respectively). In the middle third, the highest frequency artifact was presented at 15-degree (14 artifacts), followed by 10-, 20-, 5- and 0-degree (12, 10, 8, 4 artifacts, respectively). In the apical third, the highest frequency artifact was presented at 0-degree (4 artifacts), followed by 15-degree (1 artifact). Regarding the eight-direction artifact presentation, in the coronal third, artifacts were present in all directions, as shown in Figure 5A, with most found in the mesial (29 artifacts) and distal directions (25 artifacts). The artifacts observed in the cross-direction 1.57 times (69 artifacts) exceeded those in the oblique-direction (44 artifacts). In the middle third, artifacts were present in all directions, as shown in Figure 5B, the mesial direction had the highest number of artifacts (17 artifacts). The artifacts presented in the cross-direction were higher than those observed in the oblique-direction 3.8 times. In the apical third, it had a different pattern from other root levels, as the artifacts noted in the cross-direction (2 artifacts) were lower than the oblique-direction (3 artifacts), as shown in Figure 5C.

The logistic regression analysis revealed that the direction of artifact presentation significantly affected the presence of artifacts

only in the coronal third. The probability of artifact direction on the mesial ( $p<0.01$ ) and distal ( $p<0.01$ ) directions were greater than the buccal direction by 5.85 and 4.35 times, respectively. The degree of mandibular inclination and direction of artifact presentation significantly affected the presence of artifacts in the middle third. The probability of artifact presentation in mandibular inclination at 10-degree ( $p=0.04$ ) and 15-degree ( $p=0.02$ ) was 3.61 and 4.42 times greater than at 0-degree, respectively. The probability of artifact presentation on the mesial direction ( $p=0.01$ ) was 3.81 times greater than that on the buccal direction. Findings indicate that no factor affected the presence of artifacts in the apical third.

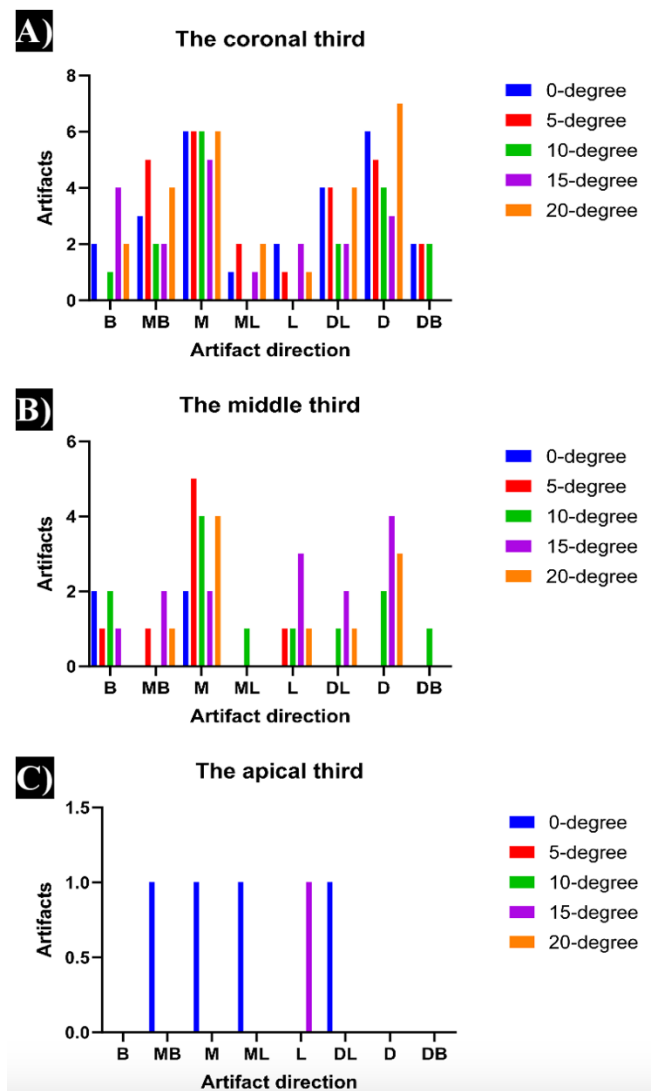


**Figure 5.** The frequency distribution of artifact presentation using the quantifying system A) The coronal third B) The middle third and C) The apical third.

## Discussion

The study thoroughly examined the influence of mandibular inclination on artifact visualization in CBCT images of endodontically-treated teeth. The scoring system assessment showed no evidence that tilting mandible was substantial enough to effect the artifact presentation, whereas the quantifying system showed considerable different results. The quantifying system assessment, which showed the probability of artifact presentation in the middle third when tilting the mandible backward at 10- and 15-degree, was consistent with the findings of Lindfors et al., who found that tilting a human skull 20-degree backward significantly improved image quality.<sup>12</sup> In contrast, Min and Kim's study indicated that tilting the mandible forward significantly reduced artifacts in the inter-implant region but had no effect on the artifact surrounding two implants.<sup>13</sup> The quantifying system revealed a higher possibility of artifacts within the middle third segment when the mandible was tilted at 10- and 15-degree. This might be explained by the anatomical structures of the mandible. When the head is tilted backward, the anterior part of the mandible increases towards bone thickness apically, causing it to move upwards.<sup>24</sup> As a result, the greater attenuation of low-energy photons leads to an increased prevalence of hypodense line artifacts. Therefore, clinician should be avoided setting head position at 10- and 15-degree backward especially when evaluating VRF in mandibular second premolar teeth by CBCT image.

The directional assessment revealed a significant effect of mandibular orientation and root canal filling materials on the artifact presentation in the middle and apical thirds according to the scoring system assessment, and the coronal and middle thirds according to the quantifying system assessment. Artifact patterns were prevalent in the cross-direction of the endodontically-treated mandibular second premolar, with a prominent incidence in the mesial and distal directions consistent with the findings by Ikubo et al. and Benic et al.<sup>10,25</sup> The artificial patterns of the incisor, canine, premolar, and molar region varied from their location along the long axis of the mandibular body. For that reason, the artifact patterns in the premolar region were present on the mesial and distal

directions. Root canal filling materials and their morphology resulted in artifacts, which were wide in the buccolingual direction and narrow in the mesiodistal direction.<sup>10</sup> Therefore, the orientation of the mandibular body determined the mesiodistal direction of the artifact presentation, whereas the configuration of the root canal filling material influenced the buccolingual direction of the artifact presentation.

A modified likubo's 4-point scoring was used to classify hypodense line artifacts according to the root penetration of the artifact. In this study, we established a restriction on the artifact thickness, limiting it to 0.5 mm, based on the range of fracture width measured by micro-CT.<sup>26-28</sup> The artificial thickness was the lowest scale for the observer to differentiate between artifact and fracture lines. The artifacts were subsequently discarded when their width exceeded 0.5 mm. The limitations of our scoring system are the observer's illusion and experience. When a light shade contacts a dark shade, illusion recognition makes the light shade brighter, and the dark shade appears darker.<sup>29</sup> The experience and expertise of the observers correlated with their ability to diagnose.<sup>7,8</sup>

A modified Johari's method was applied to define streak artifacts in CBCT images. Even though grayscale analysis can determine the initial ROI windows<sup>4,6,15,16</sup>, our preliminary investigation found discrepancies in the placement of ROIs because of the various dentin thicknesses and anatomy of the root cross-section. Calibration for ROI identification was critical, given that changes in gray value did not always indicate artifacts. We suggested Modified Johari's method and emphasized its potency in streak artifact identification. However, using modified Johari's technique in our images had two limitations. Firstly, there was a band of hypodense artifact instead of a streak artifact, which decreased the average pixel intensity along the histogram line. This band inhibited a drop in the point between the second and third peaks on the histogram graph of the coronal and middle third (Figure 3C). Also, the thin apical third dentin caused the second dropping point of the artifact presentation to vanish, resulting in the undetectable artifacts at 3.57% of the total assessment compared with the observer assessment. Secondly, the quantifying system observed eight artificial directions. The oblique line in the coronal or middle thirds frequently

overlapped with a mesial or distal artifact. A thick artifact band in the mesial or distal direction consequently affects the artifact visualization in the oblique-direction. This incident accounted for 2.50% of the total assessment (2.20% in the coronal third and 0.30% in the middle third).

Our study provides remarkable observations on the artifact nature that occurred in CBCT images of mandibular inclination, which are beneficial for root fracture diagnosis. Fractures are characterized by the sharp radiolucent line, root surface termination, and widening relevant periodontal ligament space. The artificial lines are less clear and extend over the root surface. Digital imaging technology will enhance our novel quantifying system for further detecting streak artifacts in CBCT images and providing diagnosis decisions in endodontics.

### Conclusions

The mandibular inclination influences the presentation of artifacts in CBCT images of endodontically-treated teeth. Tilting the head backward at 10- and 15-degree is prone to present more artifacts in the mandibular second premolar area in the cross-direction. Avoiding backward head tilting at 10- and 15-degree prevents more artifacts from appearing in CBCT images and enhances the diagnostic accuracy of root fractures.

### Acknowledgments

We gratefully acknowledge of Dr. Ariya Chantaramanee for the statistical advice. This study was financially supported by Faculty of Dentistry, Naresuan University, Thailand.

### Declaration of Interest

The study is original and free of conflict of interest.

### References

1. Fayad MI, Nair M, Levin MD, et al. AAE and AAOMR joint position statement: use of cone beam computed tomography in endodontics 2015 update. *Oral Surg Oral Med.* 2015;41(9):1393-1396.
2. Korobeinikova YL, Korobeinikov LS. Cone-Beam Computed Tomography in Dental Practice: Literature Review and Own Observations. *J Int Dent Medical Res.* 2023;16(4):1747-1752.
3. Oliveira MR, Sousa TO, Caetano AF, et al. Influence of CBCT metal artifact reduction on vertical radicular fracture detection. *Imaging Sci Dent.* 2021;51(1):55-62.
4. Helvacioğlu-Yigit D, Kocasarac HD, Bechara B, Noujeim M. Evaluation and reduction of artifacts generated by 4 different root-end filling materials by using multiple cone-beam computed tomography imaging settings. *J Endod.* 2016;42(2):307-314.
5. de Lima ED, de Farias Freitas APL, Suassuna FCM, Melo SLS, Bento PM, de Melo DP. Assessment of cone-beam computed tomographic artifacts from different intracanal materials on borooteed teeth. *J Endod.* 2019;45(2):209-213.
6. AlMohareb RA, Barakat RM, Mehanny M. Quantitative Analysis of Cone-Beam Computed Tomography Artifacts Induced by Nonmetallic Root Canal Filling Materials Using Different Fields of View: In Vitro Study. *Scanning.* 2022;2022:4829475. Published 2022 Feb 22. doi:10.1155/2022/4829475
7. Uysal S, Akcicek G, Yalcin ED, Tuncel B, Dural S. The influence of voxel size and artifact reduction on the detection of vertical root fracture in endodontically treated teeth. *Acta Odontol Scand.* 2021;79(5):354-358.
8. Patel S, Brown J, Pimentel T, Kelly R, Abella F, Durack C. Cone beam computed tomography in endodontics—a review of the literature. *Int Endod J.* 2019;52(8):1138-1152.
9. Nikbin A, Kajan ZD, Taramsari M, Khosravifard N. Effect of object position in the field of view and application of a metal artifact reduction algorithm on the detection of vertical root fractures on cone-beam computed tomography scans: An in vitro study. *Imaging Sci Dent.* 2018;48(4):245-254.
10. Iikubo M, Osano T, Sano T, et al. Root canal filling materials spread pattern mimicking root fractures in dental CBCT images. *Oral Surg Oral Med.* 2015;120(4):521-527.
11. Dawood A, Patel S, Brown J. Cone beam CT in dental practice. *Br Dent J.* 2009;207(1):23-28.
12. Lindfors N, Lund H, Johansson H, Ekestubbe A. Influence of patient position and other inherent factors on image quality in two different cone beam computed tomography (CBCT) devices. *Eur J Radiol.* 2017;4:132-137.
13. Min C-K, Kim K-A. Reducing metal artifacts between implants in cone-beam CT by adjusting angular position of the subject. *Oral Radiol.* 2021;37(3):385-394.
14. Luckow M, Deyhle H, Beckmann F, Dagassan-Berndt D, Müller B. Tilting the jaw to improve the image quality or to reduce the dose in cone-beam computed tomography. *Eur J Radiol.* 2011;80(3):e389-e393.
15. Salineiro FCS, Talamoni IP, Velasco SK, Barros FM, Cavalcanti MdGP. Artifact induction by endodontic materials: a CBCT analysis. *Clin Lab Res.* 2019:1-10
16. Fox A, Basrani B, Kishen A, Lam EW. A novel method for characterizing beam hardening artifacts in cone-beam computed tomographic images. *J Endod.* 2018;44(5):869-874.
17. Gholampour A, Soleymani A, Bijani A, Haghanifar S. A comparison of image artifacts with gutta-percha and different sealers on root filled teeth using cone beam computed tomography: an in vitro study. *Casp J Dent Res.* 2020;9(2):42-49.
18. Fontenele RC, Nascimento EH, Vasconcelos TV, Noujeim M, Freitas DQ. Magnitude of cone beam CT image artifacts related to zirconium and titanium implants: impact on image quality. *Dentomaxillofac Radiol.* 2018;47(6):21-28.
19. Demirturk Kocasarac H, Helvacioğlu Yigit D, Bechara B, Sinanoglu A, Noujeim M. Contrast-to-noise ratio with different settings in a CBCT machine in presence of different root-end filling materials: an in vitro study. *Dentomaxillofac Radiol.* 2016;45(5):12-20.
20. Schneider CA, Rasband WS, Eliceiri KW. NIH Image to ImageJ: 25 years of image analysis. *Nat Methods.* 2012;9(7):671-675.
21. Prewitt JM, Mendelsohn ML. The analysis of cell images. *Ann N Y Acad Sci.* 1966;128(3):1035-1053.
22. Johari M, Abdollahzadeh M, Esmaeili F, Sakhamanesh V. Metal artifact suppression in dental cone beam computed tomography images using image processing techniques. *J Med Signals sens.* 2018;8(1):12-24.

23. Landis JR, Koch G. The measurement of observer agreement for categorical data. *Biometrics*. 1977;33(1):159-174.
24. Shafizadeh M, Tehrani A, Shirvani A, Motamedian SR. Alveolar bone thickness overlying healthy maxillary and mandibular teeth: a systematic review and meta-analysis. *Int Orthod*. 2021;19(3):389-405.
25. Benic GI, Sancho-Puchades M, Jung RE, Deyhle H, Hämmerle CH. In vitro assessment of artifacts induced by titanium dental implants in cone beam computed tomography. *Clin Oral Implants Res*. 2013;24(4):378-383.
26. Huang C-C, Chang Y-C, Chuang M-C, et al. Analysis of the width of vertical root fracture in endodontically treated teeth by 2 micro-computed tomography systems. *J Endod*. 2014;40(5):698-702.
27. Makeeva I, Byakova S, Novozhilova N, et al. Detection of artificially induced vertical root fractures of different widths by cone beam computed tomography in vitro and in vivo. *Int Endod J*. 2016;49(10):980-989.
28. Gulibire A, Cao Y, Gao A, et al. Assessment of true vertical root fracture line in endodontically treated teeth using a new subtraction software—A Micro-CT and CBCT study. *Aust Endod J*. 2021;47(2):290-297.
29. Nielsen CJ. Effect of scenario and experience on interpretation of mach bands. *J Endod*. 2001;27(11):687-691.